This is the accepted manuscript made available via CHORUS. The article has been published as:

Dynamic Evanescent Phonon Coupling Across the La_{1-x}Sr_{x}MnO_{3}/SrTiO_{3} Interface

Y. Segal, K. F. Garrity, C. A. F. Vaz, J. D. Hoffman, F. J. Walker, S. Ismail-Beigi, and C. H. Ahn

Phys. Rev. Lett. **107**, 105501 — Published 30 August 2011

DOI: 10.1103/PhysRevLett.107.105501

Dynamic evanescent coupling across the $La_{1-x}Sr_xMnO_3/SrTiO_3$ interface

Y. Segal,[1,2] K. F. Garrity,[2,3] C. A. F. Vaz,[1,2] J. D. Hoffman,[1,2]
F. J. Walker,[1,2] S. Ismail-Beigi,[1,2,3] and C. H. Ahn[1,2,3]

[1]*Department of Applied Physics, Yale University, New Haven CT 06520-8284*
[2]*Center for Interface Structure and Phenomena,*
Yale University, New Haven CT 06520-8284
[3]*Department of Physics, Yale University, New Haven CT 06520-8120*

Abstract

The transport and magnetic properties of correlated $La_{0.53}Sr_{0.47}MnO_3$ ultrathin films, grown epitaxially on $SrTiO_3$, show a sharp cusp at the structural transition temperature of the substrate. Using a combination of experiment and first principles theory we show that the cusp is a result of evanescent cross-interface coupling between the charge carriers in the film and a soft phonon mode in the $SrTiO_3$, mediated through linked oxygen octahedral motions. The amplitude of the mode diverges at the transition temperature, and phonons are launched into the first few atomic layers of the film, affecting its electronic state.

PACS numbers: 63.22.Np;64.70.K-;73.50.-h;75.70.Ak;

The coupling of phonons to charge carriers is a process of key importance for a broad set of phenomena, ranging from carrier mobility in semiconductors to Cooper pairing. Phonon effects at interfaces are now emerging as a topic of great importance in the understanding and design of nano-structured materials [1]. Coupling between charge, phonons and magnetic ordering is particularly strong in the Mn oxides [2], which are used as a component in heterostructure multiferroics [3]. In these materials, localized spins and mobile carriers reside on the Mn sites, each surrounded by an oxygen octahedra. Intersite hopping occurs through orbital overlap of the Mn with neighboring oxygens, making it highly sensitive to the static orientation of the octahedra and to phonons that alter the their orientation [4]. This interplay between structure and properties has been exploited to control the electronic phase of colossal magneto-resistive (CMR) CMR films via strain, and also via coherent photoexcitation of a specific octahedra vibration mode [5].

In this Letter, we use a specially designed thin film device to isolate and characterize phonon-carrier coupling within a few atomic layers of an interface between the perovskite oxide $SrTiO_3$ (STO) and the CMR oxide $La_{0.53}Sr_{0.47}MnO_3$ (LSMO). A soft octahedral rotation phonon with a divergent amplitude in the STO couples to the corresponding mode of the LSMO film. This coupling results in a marked change in the electronic and magnetic properties, including a sharp cusp in the resistivity and a dip in the magnetic moment. The sensitivity of LSMO to octahedral orientation allows one to experimentally probe the microscopic character of this interfacial phonon coupling and compare it to first principles theory calculations describing the penetration of the soft mode into the LSMO. The thin film devices consist of LSMO films grown by molecular beam epitaxy on TiO_2-terminated STO (001) substrates. A ferroelectric oxide, $Pb(Zr_{0.2}Ti_{0.8})O_3$ (PZT) is grown on top, which is used to provide ferroelectric field effect modulation of the number and distribution of carriers in the LSMO. Details concerning fabrication and structural characterization are described elsewhere [6]. In the bulk LSMO phase diagram, the $x = 0.5$ composition separates the ferromagnetic metallic phase from an insulating antiferromagnetic phase [7]. When grown commensurate to STO, the substrate induces tensile strain in the film, which is known to stabilize an A-type antiferromagnetic metallic phase (AF-M) [8]. X-ray diffraction confirms that the films films are under tensile strain, with $c/a = 0.975$, in agreement with previous studies [8].

Transport measurements of an 11 unit cell (uc) LSMO film are shown in Fig. 1a. The

broad peak in resistivity at 250 K corresponds to a metal-insulator transition typical of LSMO. In addition, a unique feature is observed in our films: a large and sharp resistance peak centered around 108 K, which is at the temperature of the STO soft phonon peak. We observe further that the magnitude of the resistivity cusp decreases when the thickness of the film increases by a few unit cells. Indeed, in previous studies of films ≈80 uc thick, only a trace of this feature was observed [9]. This film thickness dependence implies that the strength of the mechanism creating the cusp decays quickly away from the STO/LSMO interface. We can verify this hypothesis by switching the polarization state of the PZT layer. When the PZT polarization points at the LSMO, downward, holes are repelled ("depleted") from the top layer of the LSMO, pushing the conducting region closer to the substrate. The opposite occurs in the "accumulation" state, where the carriers are pulled away from the STO/LSMO interface and towards the top part of the LSMO [3]. We find that the PZT has a pronounced effect on the cusp (Fig. 1b), making it much larger in the depletion state, in agreement with the notion of a rapid decay of the coupling mechanism into the film. We note, however, that presence of PZT is not required: the same features are observed on uncapped LSMO films. We also observe a striking dip in the magnetic moment centered around the STO transition temperature (Fig. 1a). While the majority of the LSMO is in an antiferromagnetic-metallic state, a small ferromagnetic component remains [9]. The dip in magnetic moment corresponds to a decrease in magnetic order within the ferromagnetic phase.

We attribute the transport and magnetism anomaly to a coupling between the LSMO and the phonon softening that occurs in STO around the 108 K structural transition. The Γ_{25} (111) zone edge phonon [10, 11] becomes lower in energy as the transition is approached from both temperature directions. Fig. 1c, reproduced from Ref. 10, shows the Γ_{25} phonon energy as a function of temperature. The softening leads to a diverging increase in mode occupation or amplitude. The motion associated with this mode is a rotation of the TiO_6 octahedra. Below the transition temperature, the octahedra stabilize into a rotated antiferrodistortive (AFD) configuration accompanied by a tetragonal distortion of the unit cell. Since the film is mechanically constrained to the substrate at the atomic level, motions of the TiO_6 octahedra couple to the MnO_6 ones, inducing both static and dynamic changes in their configuration.

We examine two mechanisms whereby the resistance of the LSMO layer might increase:

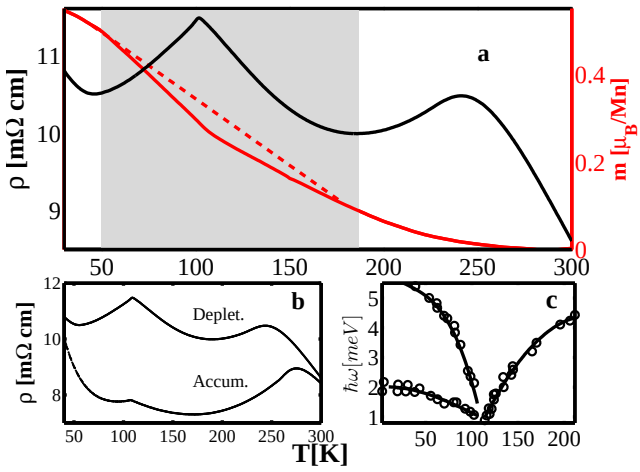

Figure 1: Enhanced carrier-phonon scattering. (a) Left axes: Resistivity of an 11 uc $La_{0.53}Sr_{0.47}MnO_3$ film showing a strong cusp at 108 K. The PZT overlayer is in the depletion state. Right axis: Magnetic moment of a 15 uc $La_{0.55}Sr_{0.45}MnO_3$ film. The moment is measured along the [100] direction under an applied magnetic field of 1kOe. A dip in the moment is observed, overlapping the temperature range of the resistivity cusp (emphasized by the gray box). The dashed line is a linear interpolation between the edges of the dip region. b) The resistivity of the 11 uc film for the two polarization states of the PZT layer. c) Energy of the Γ_{25} phonon mode in STO, showing the softening around the STO transition temperature (after Ref. 10). Lines are a guide to the eye. Below the structural phase transition temperature the mode splits due to the breaking of cubic symmetry.

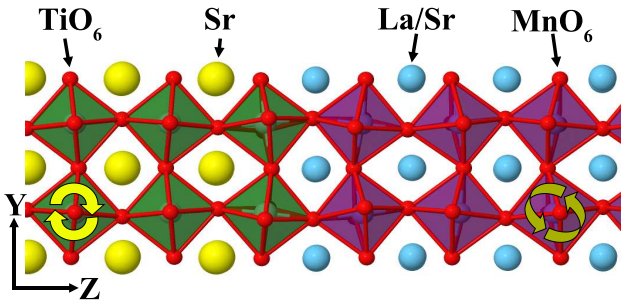

Figure 2: Side view of the STO/LSMO interface geometry. The plot shows calculated ground-state atomic positions. Away from from the interface, the STO is fixed to have bulk-like octahedral rotations around the x axis (into the page). The LSMO geometry at the interface is modified by the STO; however, the LSMO relaxes to its bulk-like octahedral rotations around both in-plane axes within 2-3 unit cells.

(i) static changes of the LSMO structure causing a change of electronic band parameters; and (ii) decreased carrier relaxation times due to enhanced phonon scattering, i.e. a dynamic effect. The static and dynamic contributions are reflected in the expression for the conductivity in the relaxation time approximation $\sigma_{ij} \propto \tau m_{ij}^{-1}$, where τ is the relaxation time and m_{ij}^{-1} is the reciprocal effective mass tensor [12].

To treat the temperature-dependent character of the coupling phenomena, we perform finite temperature simulations by building a classical model of the energetics of the system as a function of oxygen displacements. Our model includes harmonic coupling between oxygens, 4^{th} order on-site anharmonic terms to stabilize the symmetry breaking, and lowest order coupling between oxygen displacements and stress [13]. Model parameters are obtained via density functional theory calculations using the spin-polarized PBE GGA functional [14] and ultrasoft pseudopotentials [15]. Ground states for both bulk strained LSMO (using the virtual crystal approximation [16]) and the LSMO/STO system are calculated, reproducing the experimental A-type ordering. In addition, the ground state calculations show how the static octahedral orientation changes continuously in going from substrate to film (see Fig. 2), as was recently shown in a similar theoretical study [17]. The harmonic interatomic force constants are calculated with DFT perturbation theory (DFPT) [18], and the remaining parameters are fit to strained bulk calculations. We then perform classical Monte Carlo sampling on this model in a periodic box. The box contains $10 \times 10 \times 100$ perovskite unit cells composed of 60 STO and 40 LSMO unit cells in the z direction. See the supplementary text for further details [19].

To evaluate the role of static structural changes, we compute the conductivity tensor of bulk strained LSMO for the static octahedra rotation angles obtained from the Monte-Carlo model. The conductivity is calculated from direct first principles evaluation of the reciprocal effective mass tensor by summing over all bands at the Fermi energy [12, 19]. The upper bound of conductivity change is estimated by using the angles at the LSMO/STO interface, which change the most due to the substrate-film coupling. We find that the static coupling effect appears only below the phase transition temperature. The phase transition causes the octahedra angles in the LSMO to increase by $\sim$0.1 degrees; however, the magnitude of the resulting change in conductivity is too small to account for the experimental findings. The computed Mn-O-Mn hopping elements change only by 1-2% due to static structural changes, while the experimental conductivity changes by more than 10%.

Because the static structural change manifests itself only below 108 K and does not yield a large enough change in conductivity, we examine whether the Γ_{25} phonon mode extends into the LSMO and causes dynamic carrier scattering. We compute the oxygen-oxygen correlation matrix $c_{ij} = \langle x_i x_j \rangle - \langle x_i \rangle \langle x_j \rangle$, where x_i are the oxygen displacements from their equilibrium pseudocubic positions. We find that near the STO phase transition, the correlation length in STO diverges, as expected. Furthermore, oxygen motions in the interfacial LSMO layers become correlated with those deep in the STO (Fig. 3a), demonstrating that STO soft phonons extend into the LSMO. We quantify this relation more precisely by extracting the dominant eigenvectors of the correlation matrix, which are the softest phonon modes in the finite-temperature harmonic system [19]. Fig. 3b shows the lowest frequency eigenvector: it decays exponentially into the LSMO with a decay length of 2.3 unit cells. While it is tempting to use the phonon of the T=0 broken symmetry AFD ground state to understand the evanescent behavior, there is no guarantee on the accuracy of this approach since the interatomic spring constants are temperature-dependent: some are so strongly dependent that key phonon frequencies go to zero about T_c. Our approach can extract phonon behavior at temperatures where the cubic high-symmetry structure is the minimum of the free energy but not of the T=0 energy.

Building upon our theoretical results, we use a simple model to fit the experimental resistivity data [19]. In brief, the scattering in layer z due to the soft mode is $cne^{-2z/\lambda}$, where n is the Γ_{25} phonon's Bose-Einstein occupation number evaluated using the phonon energies in Fig. 1c; c is a conversion factor from n to resistivity (linearly related in phonon scattering theory [20]); and λ is the decay length of the induced octahedra motion amplitude ($\lambda/2$ is the decay length for the phonon number). The total conductivity is obtained by summing over the film layers [19]. This model describes the experimental data well, as shown in Fig. 4, and yields a decay length of 1.8 uc, in good agreement with theory. This model corroborates our attribution of the resistivity cusp to coupling of the divergent Γ_{25} mode into the LSMO, where it strongly scatters the carriers by disturbing the Mn-O-Mn hopping path.

The phonon coupling picture also provides a qualitative explanation of the dip in magnetic moment, when phonon-magnon interactions are considered. For the manganites, it has been shown theoretically [21] that when phonons involving Mn or O distortions are added to the Heisenberg Hamiltonian, the magnon spectrum is softened. The phonons injected from the substrate cause a softening of the magnon spectrum in the LSMO, with maximal softening

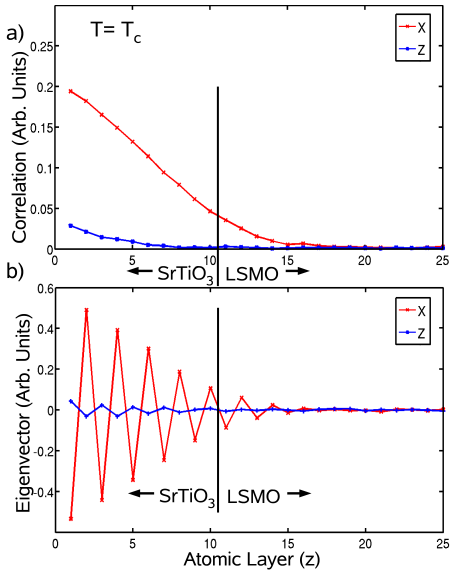

Figure 3: DFT/Monte Carlo results of phonon transfer from STO to LSMO. a) Absolute magnitude of the correlation function of oxygen displacements with those deep in the STO as a function of layer number at $T = T_C$. x and z indicate displacements stemming from octahedral rotation around the x and z axis, respectively. (The y component is equal to x by symmetry). b) x and z components of the lowest frequency eigenvector at $T = T_C$. The layer-to-layer sign changes reflect the AFD nature of the oxygen displacments.

occuring at the STO transition. Magnon occupation increases with spectrum softening, leading to a reduction in the magnetic moment. The overlap between the temperature range of the transport cusp and the moment dip is striking (Fig. 1a), strongly suggesting that they are both driven by Γ_{25} phonon softening. A quantitative treatment and verification of this magnon-softening picture is a research challenge beyond the scope of this letter.

Previous work on the influence of the STO transition on manganite films dealt with effects attributed to the appearance of a and c domains in the STO and the resulting change in the strain state of the film below the transition temperature [22–24]. In the current work, we find that effects appear both above and below the transition temperature and correspond to the temperature range of phonon softening. In addition, the short decay length that we find does not agree with a strain-mediated phenomenon. The LSMO remains strained to the substrate up to a thickness of at least 80 uc [8], so that changes related to strain should be evident at these thicknesses as well. These two facts preclude the strain configuration of the STO below the transition as the source of the cusp. To further verify that the cusp feature

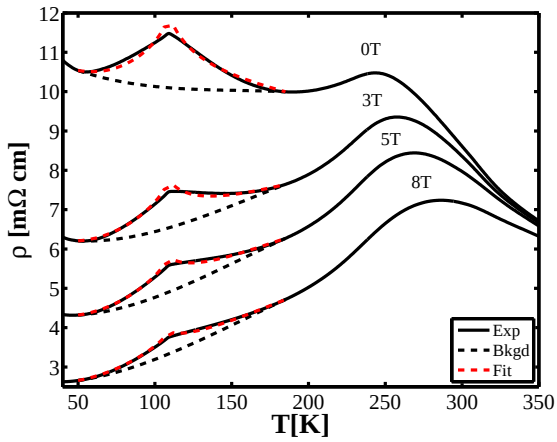

Figure 4: Resistivity of an 11 uc film of $La_{0.53}Sr_{0.47}MnO_3$ as a function of temperature, for several out-of-plane magnetic field values. The PZT overlayer is in the depletion state. Black dashed lines are interpolations excluding the cusp, and the red dashed lines are fits to Γ_{25} phonon coupling.

is independent of the a/c domain structure formed in the STO, we applied an electric field of 2×10^5 V/m using a back gate on the substrate. This field should break the symmetry between a and c domains and lead to a different domain structure compared to a zero field case. No difference in resistivity is observed with and without the electric field.

Our observation of phonon-carrier coupling illuminates a key feature of conduction in LSMO. The coupling manifests itself strongly near the $x = 0.5$ composition, while films of similar thickness at the $x = 0.2$ composition [3] show a resistivity cusp that is much smaller in magnitude. We relate this effect to an increased carrier coupling to the Γ_{25} phonon in the AF-M phase of the LSMO. In this phase, the Mn $d_{x^2-y^2}$ e_g orbital is occupied, while the $d_{3z^2-r^2}$ orbital is depopulated [25]. This configuration causes the carriers' wavefunctions to be concentrated on the xy MnO_2 planes, which underpins the 2D character of metallicity and ferromagnetism in this phase, in contrast to the 3D character of the $x = 0.2$ to 0.4 composition range. The transport measurements of our thin films probe carrier hopping in the x and y directions. Perturbation of the bridging oxygen positions due to the Γ_{25} phonon will have a larger scattering effect on carriers in the AF-M phase compared to the 3D FM phase. This is because in the AF-M case, the electron density case is concentrated closer to the perturbed oxygens in the xy plane, through which the conduction occurs. This configuration also explains why an out-of-plane magnetic field reduces the effect of the phonon coupling, as can be seen in Fig. 4. The magnetic field causes the Mn spins

to cant so that they are partially aligned out-of-plane. This canting allows for some inter-plane hopping and reduces the confinement of carriers to the xy MnO_2 planes, similar to the "spin valve" effect in A-type $Nd_{0.45}Sr_{0.55}MnO_3$ [26]. The above arguments are qualitative. A quantitative *ab initio* treatment of the difference in sensitivity of the AF-M and FM phases to Γ_{25} phonons is at present underway. A full rigorous treatment, including the effect of canting, is a research challenge for the field.

In conclusion, we show how a single phonon mode originating in the substrate extends across an epitaxial interface. The effects of this coupling are amplified by the properties of both materials: phonon softening in the substrate causes the phonon amplitude to diverge, while the LSMO's electronic phase and charge distribution are tuned using strain and a ferroelectric gate.

This work was supported by the National Science Foundation under Contract MRSEC No. DMR-0520495, DMR-1006265, and FENA. Computational resources were provided by Yale High Performance Computing, partially funded by grant CNS 08-21132 and by TeraGrid/NCSA under grant number TG-MCA08X007.

[1] D. G. Cahill et al., J. Appl. Phys. **93**, 793 (2003).

[2] M. B. Salamon and M. Jaime, Rev. Mod. Phys. **73**, 583 (2001).

[3] C. A. F. Vaz, J. Hoffman, Y. Segal, J. W. Reiner, R. D. Grober, Z. Zhang, C. H. Ahn, and F. J. Walker, Phys. Rev. Lett. **104**, 127202 (2010).

[4] Y. Tokura, Rep. Prog. Phys. **69**, 797 (2006).

[5] M. Rini, R. Tobey, N. Dean, J. Itatani, Y. Tomioka, Y. Tokura, R. W. Schoenlein, and A. Cavalleri, Nature (London) **449**, 72 (2007).

[6] C. A. F. Vaz, Y. Segal, J. D. Hoffman, F. J. Walker, and C. H. Ahn, J. Vac. Sci. Technol. B **28**, C5A6 (2010).

[7] O. Chmaissem, B. Dabrowski, S. Kolesnik, J. Mais, J. D. Jorgensen, and S. Short, Phys. Rev. B **67**, 094431 (2003).

[8] Y. Konishi, Z. Fang, M. Izumi, T. Manako, M. Kasai, H. Kuwahara, M. Kawasaki, K. Terakura, and Y. Tokura, J. Phys. Soc. J. **68**, 3790 (1999).

[9] T. S. Santos, S. J. May, J. L. Robertson, and A. Bhattacharya, Phys. Rev. B **80**, 155114

(2009).

[10] J. F. Scott, Rev. Mod. Phys. **46**, 83 (1974).

[11] P. A. Fleury, J. F. Scott, and J. M. Worlock, Phys. Rev. Lett. **21**, 16 (1968).

[12] N. W. Ashcroft and N. D. Mermin, *Solid State Physics* (Brooks Cole, 1976).

[13] W. Zhong and D. Vanderbilt, Phys. Rev. Lett. **74**, 2587 (1995).

[14] J. P. Perdew, K. Burke, and M. Ernzerhof, Phys. Rev. Lett. **77**, 3865 (1996).

[15] D. Vanderbilt, Phys. Rev. B **41**, 7892 (1990).

[16] L. Bellaiche, D. Vanderbilt, Phys. Rev. B **61**, 7877 (2000).

[17] J. M. Rondinelli and N. A. Spaldin, Phys. Rev. B **82**, 113402 (2010).

[18] P. Giannozzi, S. de Gironcoli, P. Pavone, and S. Baroni, Phys. Rev. B **43**, 7231 (1991).

[19] See Supplementary Material at http://link.aps.org/ for details of the calculations.

[20] J. M. Ziman, *Electrons and Phonons*, International Series of Monographs in Physics (Oxford Press, 1960).

[21] L. M. Woods, Phys. Rev. B **65**, 014409 (2001).

[22] V. K. Vlasko-Vlasov, Y. K. Lin, D. J. Miller, U. Welp, G. W. Crabtree, and V. I. Nikitenko, Phys. Rev. Lett. **84**, 2239 (2000).

[23] M. Ziese, I. Vrejoiu, A. Setzer, A. Lotnyk, and D. Hesse, New J. Phys. **10**, 063024 (2008).

[24] M. Egilmez, M. M. Saber, I. Fan, K. H. Chow, and J. Jung, Phys. Rev. B **78**, 172405 (2008).

[25] Z. Fang, I. V. Solovyev, and K. Terakura, Phys. Rev. Lett. **84**, 3169 (2000).

[26] H. Kuwahara, T. Okuda, Y. Tomioka, A. Asamitsu, and Y. Tokura, Phys. Rev. Lett. **82**, 4316 (1999).